Title

Single-shot large field of view Fourier transform holography with a picosecond plasma-based soft X-ray laser.

Journal
Optics Express, 28(24)

ISSN
1094-4087

Authors
Wang, Shoujun
Rockwood, Alex
Wang, Yong
et al.

Publication Date
2020-11-23

DOI
10.1364/oe.409815

Peer reviewed

Research Article | Vol. 28, No. 24 / 23 November 2020 / Optics Express 35898

Optics EXPRESS

Single-shot large field of view Fourier transform holography with a picosecond plasma-based soft X-ray laser

SHOUJUN WANG,[1,4] ALEX ROCKWOOD,[2] YONG WANG,[1] WEI-LUN CHAO,[3] PATRICK NAULLEAU,[3] HUANYU SONG,[1] CARMEN S. MENONI,[1] MARIO MARCONI,[1,5] AND JORGE J. ROCCA[1,2,6]

[1] *Department of Electrical and Computer Engineering, Colorado State University, Fort Collins, Colorado 80523, USA*
[2] *Department of Physics, Colorado State University, Fort Collins, Colorado 80523, USA*
[3] *Center for X-ray Optics, Lawrence Berkeley Laboratory, Berkeley, California 94720, USA*
[4] *shoujun.wang@colostate.edu*
[5] *mario.marconi@colostate.edu*
[6] *jorge.rocca@colostate.edu*

Abstract: It is challenging to obtain nanoscale resolution images in a single ultrafast shot because a large number of photons, greater than 10^{11}, are required in a single pulse of the illuminating source. We demonstrate single-shot high resolution Fourier transform holography over a broad 7 µm diameter field of view with ~ 5 ps temporal resolution. The experiment used a plasma-based soft X-ray laser operating at 18.9 nm wavelength with nearly full spatial coherence and close to diffraction-limited divergence implemented utilizing a dual-plasma amplifier scheme. A Fresnel zone plate with a central aperture is used to efficiently generate the object and reference beams. Rapid numerical reconstruction by a 2D Fourier transform allows for real-time imaging. A half-pitch spatial resolution of 62 nm was obtained. This single-shot nanoscale-resolution imaging technique will allow for real-time ultrafast imaging of dynamic phenomena in compact setups.

1. Introduction

High-resolution imaging techniques enable important applications in material science, biology and medicine. The achievable spatial resolution, r, scales linearly with the incident wavelength λ, and inversely with the numerical aperture of the optical system, NA, according to $r = (k \cdot \lambda)/NA$, where k is a factor that depends on the illumination [1]. Consequently, an approach to improve the resolution is the use of shorter wavelengths. Particular interest is the range of extreme ultraviolet (EUV) and soft X-ray (SXR) region where highly coherent beams are generated at several accelerator-based national facilities [2–5], as well as by more compact sources [6–11]. Microscopes that combine zone plate (ZP) lenses with compact plasmas-based discharge pumped [12,13] and laser-pumped [14–16] EUV/SXR lasers have produced images with up to 38 nm resolution in transmission mode [16] and 55 nm in reflection mode [14]. Sequential EUV ZP imaging of a magnetic probe oscillating at 318.6 kHz was demonstrated with ~ 1 ns temporal resolution and 54 nm spatial resolution using a 46.9 nm capillary discharge laser [17]. Alternative it is possible to eliminate the need for optics by measuring the far field diffraction pattern of the object. This is the approach of Fourier transform holography (FTH) [18] and coherent diffractive imaging (CDI) [19]. However, a challenge is to be able to obtain single shot images with high spatial and temporal resolution, a topic of high current interest particularly in SXR and XUV spectra region [13,17,20–25].

#409815 https://doi.org/10.1364/OE.409815
Journal © 2020 Received 10 Sep 2020; revised 28 Oct 2020; accepted 28 Oct 2020; published 11 Nov 2020

In CDI, the real-space image is retrieved from the coherent diffraction pattern of the object alone. The phase of the object wave can be obtained by employing iterative phase retrieval. CDI and the reconstruction require extensive computations that do not allow for real-time imaging. In contrast, the FTH hologram is recorded as the interference between the diffracted wave by the object and a known reference wave. The object can be numerically reconstructed in a fast, simple and robust manner via a 2D Fast Fourier Transformation (FFT) of the hologram, making FTH an ideal method for high-resolution real-time imaging.

In FTH there are several factors that play in determining the achievable spatial resolution and the field of view (FOV). Since the image is the convolution of the object and reference waves, high spatial resolution requires a delta function-like reference. This means the spatial resolution is limited by the size of the reference point source, that in turn relies on the fabrication techniques currently available to create a small pinhole aperture. However, a small pinhole decreases the intensity of the reference beam due to its lower throughput. The immediate consequence is that the reference and the object waves have very dissimilar intensities, producing interference fringes with very poor visibility. At the same time, a long exposure time, is necessary to increase the hologram signal-to-noise ratio (SNR). A resolution of ~50 nm has been demonstrated using a synchrotron X-ray beamline with typical exposure times of 10 s per frame [26]. A way to improve the SNR is utilizing multiple reference sources, to extend the detection limit of FTH [27]. Replacing the reference pinhole with a uniformly redundant array also showed improvement in the resolutions to 44 nm [28]. On the other hand, to image a large object it is necessary to have a wide FOV, which generates high spatial frequency fringes. Consequently, the numerical aperture and the detector's pixel size limit the maximum spatial frequency that can be recorded and therefore sets a limit on the spatial resolution. Extended FOV FTH spanning 180 µm has been demonstrated by applying spatial multiplexing using a filtered soft X-ray beam originating from an undulator source [29]. Such full-field of view imaging needs long exposure time and/or a large photon flux that is only achievable at synchrotrons and Free-Electron Lasers (FELs) [30].

The limited access to large-scale facilities is a powerful motivation to bring high-resolution X-ray imaging to a table-top scale system. The successful demonstration of an X-ray nanoscale imaging with high spatial and temporal resolution in a large FOV at table-top scale will provide an attractive tool that can have a significant impact. Such compact table-top system could use sources that include high harmonic generation (HHG) and plasma-based SXR lasers. With HHG CDI has been successfully demonstrated at table-top scale [31,32] with a best resolution of 22 nm [33], but in a single shot a resolution of 119 nm was reported [21]. FTH using a HHG source also been demonstrated with a resolution of 53 nm [34]. However, the limited photon flux per-pulse of HHG sources requires long exposure times. For the same reason, the imaged area was limited to less than 9 square micrometers. In 2018 by increasing HHG repetition rate to 100 kHz, a half-pitch resolution of 34 nm was obtained with a reduced exposure time of tens of seconds. However, the imaged object area was only 0.075 μm^2 [35].

In contrast, plasma-based SXR lasers have the advantage of a much larger number, $\sim 10^{11}$, photons per-pulse, which makes it possible to demonstrate single-shot FTH. The first hologram obtained with a plasma based SXR laser was a Gabor hologram [36]. More recently a resolution of 87 nm has been obtained using a FTH setup with a FOV of 9 μm^2 [37]. Using an EUV capillary discharge laser source operating at 46.9 nm wavelength a spatial resolution of 169 nm was obtained in a single laser pulse with temporal resolution of $\approx$1ns [22,38]. Single-shot CDI with 180 nm resolution using a 18.9 nm Ni-like Mo SXR laser was also reported [39].

In this work, we demonstrate single-shot picosecond resolution FTH using a setup that a custom-made ZP with a central aperture that plays the role of a beam splitter. The ZP generates both the point source for the reference source (third order focus) and the illuminating (central opening) beams. In contrast to FTH in which a pinhole produces a reference beam, this geometry increases by orders of magnitude the flux and therefore the area of the object that can be recorded by equalizing the intensities of the object and reference beams. A similar experimental setup was used before with a synchrotron source [18]. Moreover, by employing a dual-plasma amplifier laser scheme the spatial coherence and beam divergence of the SXR lasers source are dramatically improved. A large number of coherent photons were concentrated on the ZP area generating high contrast holograms which is essential for single-shot large FOV FTH. A half-pitch resolution of up to 62 nm was achieved with single-shot SXR laser illumination, yielding a temporal resolution of 5 ps. The area imaged was 38.5 μm^2 i.e. near an order of magnitude larger than formerly reported experiments with SXR lasers [37] and more than 500 times the area in experiments using HHG sources [35]. Finally, mounting the ZP beam splitter and the object in separate motorized high precision translation stages allowed for the inspection of the object at different planes along the optical axis by displacing the point source reference plane.

2. Experimental setup

The experimental setup is illustrated in Fig. 1. A highly coherent Ni-like Molybdenum SXR laser emitting at 18.9 nm wavelength illuminates a custom-made condenser ZP that is used as a beam splitter. The use of a ZP serves two purposes. First, it gathers a larger fraction of the illuminating beam to allow for a better intensity equalization between the object and the reference beams, which in turn overcomes the object size limitations in the mask-based FTH. Second, by tailoring the design of the ZP a tens of nanometer diameter focal point can be achieved. The central aperture of the ZP allows the SXR laser beam to pass through and illuminates the object area located in a downstream plane. The remaining part of the beam impinging the ZP is focused into a small pinhole placed in the same plane as the object to create the reference beam for the FTH. The scattered beam in the object and the reference beams interfere in a CCD camera that records the hologram. Unlike in the mask-based FTH, where the resolution is limited by the reference pinhole size, the spatial resolution in this setup is defined by the focal spot size of the zone plate. The pinhole located in the object plane serves the only purpose to block the other diffraction orders produced by the ZP that would blur the interference pattern. Thus, the size of the pinhole is not the main factor that affects the resolution of the reconstruction. The distance between the high transmission orifice where the sample is located and the pinhole that transmits the refence point source was selected to assure that the interference fringes are resolved in the image plane with a CCD with the pixel size of 13.5 µm. The size of the high transmission sample hole was selected to assure that the autocorrelation of the object is not superposed with the cross correlation when the FFT in performed in the reconstruction process.

The experiment used an available ZP originally designed and fabricated at Lawrence Berkeley National Laboratory for 46.9 nm wavelength. Details of the fabrication process of the zone plate can be found in Ref. [40]. The self-standing structure allows for maximum transparency of the SXR laser beam. The ZP has 623 self-standing zones with an outer diameter of 500 µm, an outer zone width of 200 nm and a center aperture of 30 µm. The focal spot size is directly related to the Rayleigh resolution and gives an achievable resolution of $1.22\Delta r/n_{order}$, where Δr is the outer zone width and n_{order} is the order number [1]. By using a higher diffraction order, it is possible to achieve a smaller focal spot and larger NA, increasing the FTH resolution. In this work we use the 3rd order of the ZP which gives a calculated spot size of 81 nm, a NA of 0.14 and a focal length of 1.78 mm for λ=18.9 nm. However, the drawback of using a higher order is that the diffraction efficiency of the ZP decreases with the order number. In a self-standing ZP, half the incident light is lost due to absorption. The zero order has about 25% of the incident light, each one of the 1st orders have around 10% of the light while the 3rd order encompasses around 1% of the incident light [1]. The low diffraction efficiency at 3rd order is mitigated by using a coherent SXR laser source with high photon flux, which is described below. Although the zone plate was not optimized for 18.9 nm, it provides a reasonable alternative to create a bright point reference source using the third order focal point.

Optics EXPRESS

The ZP focal spot was positioned inside the pinhole in the sample mask using an actuator driven 3-axis stage. The object was placed at the focal distance of 1.78 mm away from the ZP, supported by the same foil that contains the pinhole that is motorized by a 3-axis stage. The sample holder was implemented with a 50 nm thick Si_2N_3 membrane coated with 5 nm Cr and 30 nm Au layers to enhance the absorption. A 7 µm diameter region was left without coating to preserve a region with higher transmission (approximately 57%) for the 18.9 nm SXR laser beam in which the sample is placed. Additionally, a 3 µm hole was defined in the membrane to allow for the passage of the reference beam produced by the 3^{rd} order focus of the ZP. The pinhole for the reference beam was located at 8 µm from the center of the sample region. The object consisted of an ensemble of Ag nanowires, diameter varied from 180 nm to 120 nm, that were randomly placed over the high transmission orifice in the sample holder. A Ag nano-wire suspension was spin coated on top of the sample holder membrane in such a way that nanowires

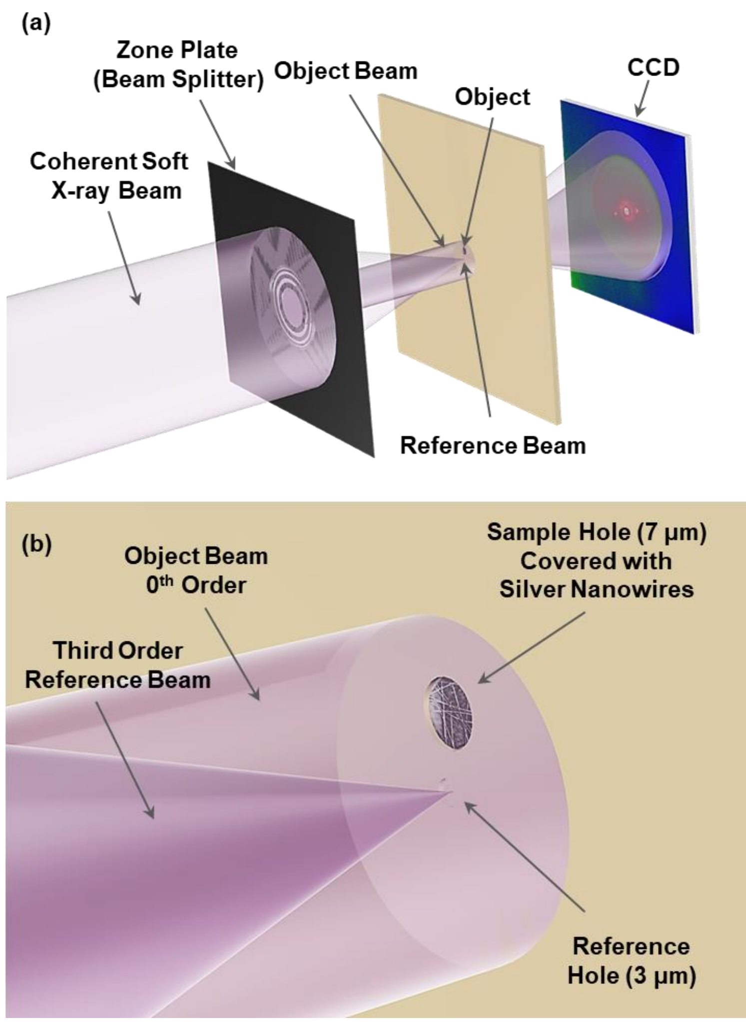

Fig. 1. (a) Schematic representation of the Fourier holography setup. A zone plate is used as a beam splitter. The mask contains a hole to define the reference beam and a semitransparent area to support the sample. The recording is performed with a CCD. (b) Zoom of the sample plane showing beam that illuminates the sample and the refence beam.

were randomly deposited over the 7 µm diameter high transmission region. Scanning electron microscope (SEM) images of two samples prepared by this procedure are shown in Fig. 2. An Andor X-ray CCD with an array size of 2048 × 2048, 13.5 µm square pixels was used to capture the diffracted light downstream. The CCD was placed 50 mm away from the sample.

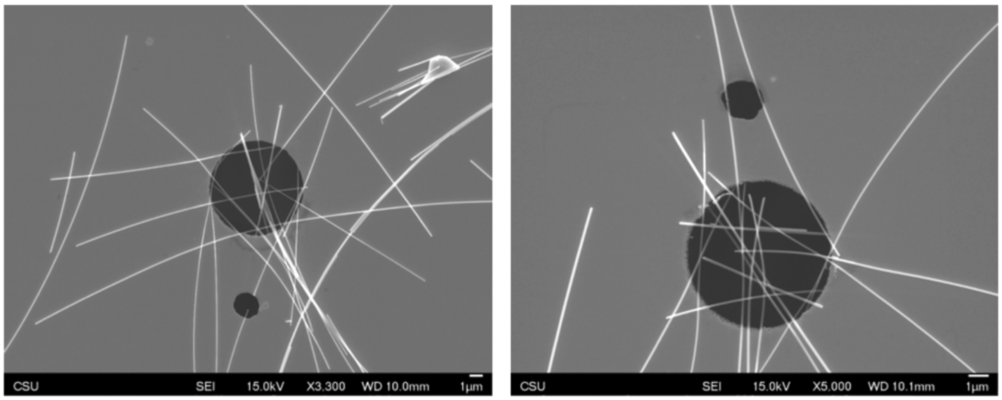

Fig. 2. SEM images of the two samples used in the experiment. Each sample consists of an opaque membrane with a 7µm hole where silver nanowires were placed. The membrane contains a 3µm diameter hole for the reference beam separated by a center to center distance of ~8 µm.

3. Plasma based SXR laser illumination source with high spatial coherence

The implementation of soft X-ray FTH requires a coherent source. The plasma-based SXR lasers operate in the amplified spontaneous emission (ASE) regime that typically produce beams with insufficient spatial coherence for holography. For this reason, most of the holography experiments reported used only a small fraction of the SXR laser beam, which significantly decreases the photon flux and consequently limits the imaging area. To achieve near full spatial coherent SXR laser beam necessary for holographic recording we choose the double plasma configuration first demonstrated by M. Nishikino et al. [41]. With this particular configuration of two amplifiers, a seeding plasma and an amplifier plasma column, we produced ~ 2×10^{11} photons per shot at λ=18.9 nm beam with practically full spatial coherence, that is suitable for single shot FTH imaging.

The SXR laser scheme used in our work is shown schematically in Fig. 3. Two Mo slab targets of the same length were located on the same axis and were pumped with similar laser pulses. Each target was irradiated with a two pulse pump laser sequence from a Ti:sapphire laser [42], which has the capability running at the repetition rate of up to 3.3 Hz. Each pump pulse sequence consisted of a 300 ps normal incidence pre-pulse that creates a plasma with a degree of ionization close to Ni-like stage, followed by a 5 ps pulse impinging at a grazing incidence of 22°. The short pulse rapidly heats the electrons to produce a transient population inversion by collisional electron impact excitation. The short pulse pump beam was focused onto lines of 15 µm width and 5.5 mm length on each target. A step mirror set was used to generate a traveling-wave excitation velocity of 1.0 c [11]. The seed and the amplifier plasma columns were separated by 24.5 mm. This distance assures that only a small fraction of the seed wavefront is further amplified in the second plasma. This results in a high spatial coherence amplified beam due to the inherent spatial filtering exerted by the small cross-sectional area (~20µm in diameter) of the gain region. The two amplifier columns were pumped with an adequate delay for the seed pulse to reach the amplifier column at the peak of the gain. The SXR laser beam was

Optics EXPRESS

finally filtered with Al foils to avoid saturating the detector and to eliminate visible plasma light. An X-ray CCD camera placed 815 mm away from the amplifier plasma recorded the SXR laser far-field pattern which was integrated to measure the pulse energy.

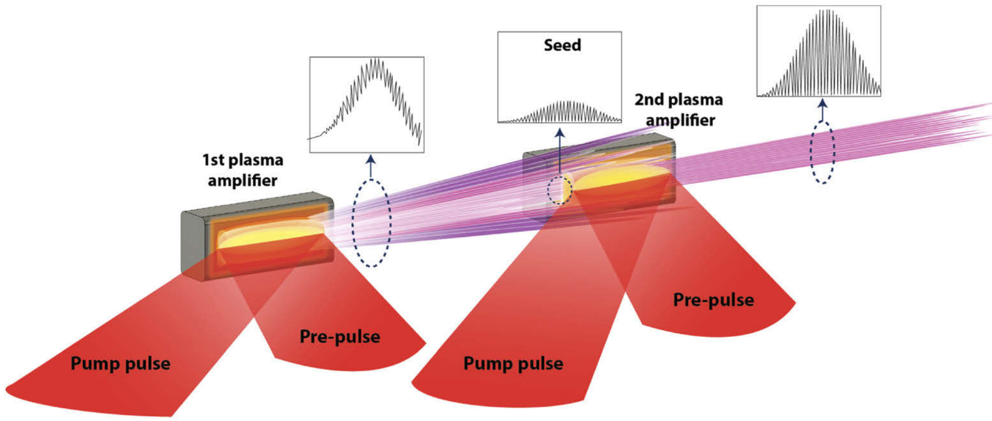

Fig. 3. Schematic depiction of the two-plasma self-seeded SXR laser amplifier setup for the generation of a beam with nearly full spatial coherence. The small cross section of the gain region in the amplifier plasma acts like a spatial filter ensuring the full spatial coherence of the seed pulses. Each plasma is pumped by a sequence of a 300 ps normal incidence pre-pulse followed by a 5 ps main pulse at 22° gracing incidence.

Figure 4 compares typical far-field patterns corresponding to the unseeded and the seeded Ni-like Mo 18.9 nm SXR lasers. The SXR laser beam from the first plasma amplifier shows a typical divergence of 5 mrad. In contrast, the dual-plasma self-seeded SXR laser yields a beam characterized by a small near-diffraction limited 0.66 mrad full width at half maximum (FWHM) divergence.

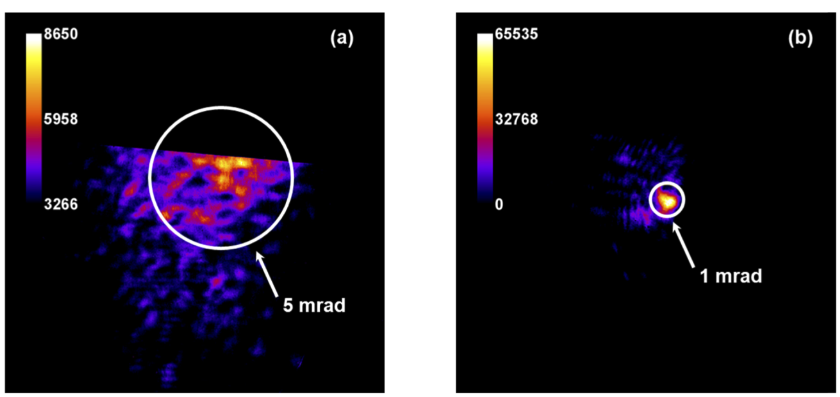

Fig. 4. Unseeded (a) and seeded (b) Ni-like Mo 18.9 nm SXR laser far field patterns. The pseudo-color scales of the two images shows the intensity of seeded beam is several times larger than that of the unseeded beam.

A Young's double-slit experiment was conducted to evaluate the transverse coherence of the two-stage SXR laser. A mask with 10 μm wide double slits separated by 50 μm was inserted 145 mm away from exit of the plasma amplifier, covering most of the beam. The interference fringe pattern was recorded by a CCD. Figure 5 shows a typical interference image for the seed SXR laser beam. The high visibility of the interference fringes is an indication of a practically fully transverse coherent beam [43].

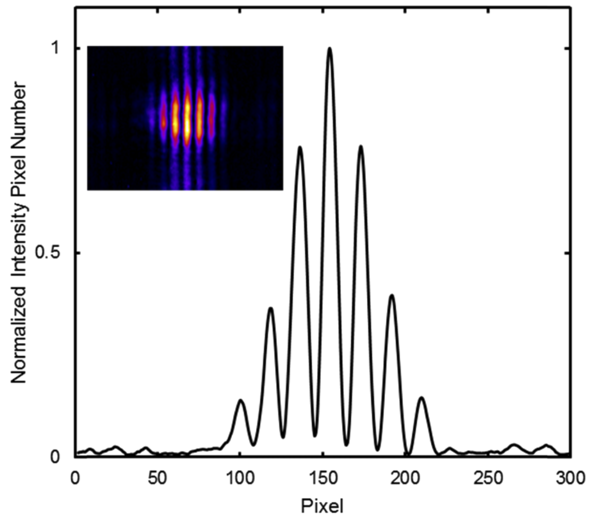

Fig. 5. Interference pattern of 18.9 nm beam from the dual-plasma SXR laser showing near full spatial coherence.

The typical linewidth of the transient collisional Ni-like Mo 18.9 nm laser was previously measured to be $\Delta\lambda/\lambda \approx 1.3\times10^{-5}$ [44], corresponding to a temporal coherence length of ~ 640 µm. The pulse duration of this type of Ni-like collisionally excited grazing incidence plasma-based SXR lasers was measured to be ~5 ps using a streak camera [45]. The pulse energy of the seeded amplified was measured to be about 10 µJ. This highly coherent bright SXR laser was directed toward the ZP by a flat gold coated mirror at grazing incidence. The distance between the SXR laser source and the ZP was set to be 815 mm such that the seeded beam expands sufficiently to cover the entire ZP.

4. Results and discussion

A typical recorded hologram is shown in Fig. 6. The hologram was digitally multiplied by a mask to zero out the regions outside the zone with interference fringes to reduce the influence of noise. An FFT of the data finally resulted in an image of the object at the plane of the ZP third order focus. Figure 7 compares picosecond resolution single-shot images of nanowire ensembles to those obtained from the same samples using a scanning electron microscope.

A typical cross section of the top image is shown in Fig. 8, corresponding to the small red segment of a 135 nm diameter Ag nanowire indicated in Fig. 7(b). The resolution is measured to be 62 nm using the 10% to 90% knife edge criterion [1].

To assess the spatial resolution, we used the 10% to 90% knife edge criterium. Considering that the reconstruction of the image is produced by a 2D FFT operation, the image is the result of the convolution of the object with a point source that in our case we assumed to be Gaussian with a FWHM=81 nm. Convolving a Gaussian function with a step function, produces also a Gaussian profile. This Gaussian profile is the image that we can expect to obtain after the reconstruction from a hard-edge object. The spatial spread for an 81 nm FWHM Gaussian to rise from 10% to 90% of its peak value is Δx=58 nm which is consistent with the experimental results we obtained (62 nm).

The utilization of the ZP to create a more intense point reference source allowed for a comparatively large field of view of 38.5 µm^2. The imaged area could be further increased

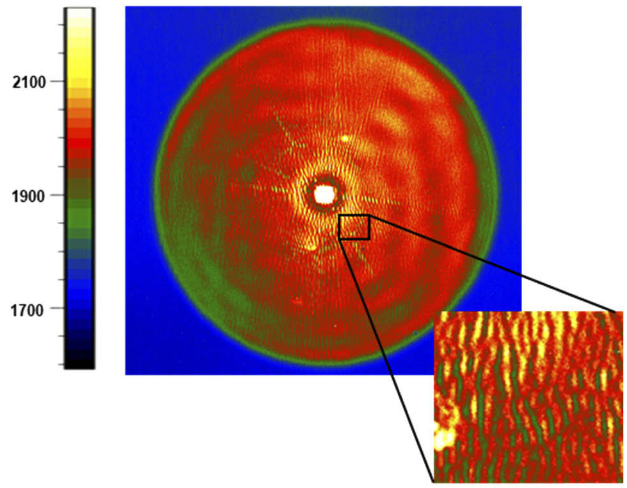

Fig. 6. Typical single shot SXR laser Fourier holography image with a zoom of the fringe pattern.

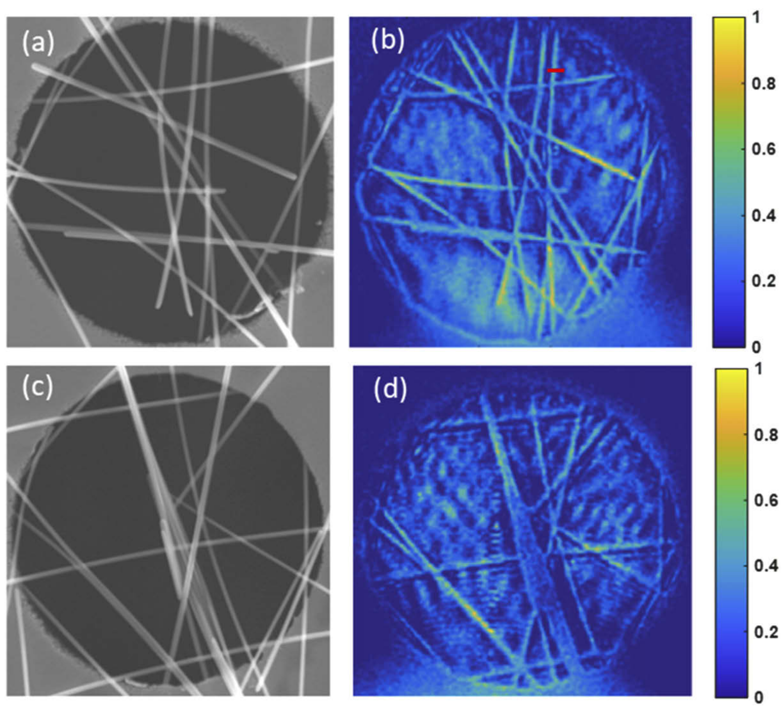

Fig. 7. Electron microscope image (a), (c) and corresponding single shot holographic images (b), (d) of the silver nanowires over a 7 µm diameter hole.

Optics EXPRESS

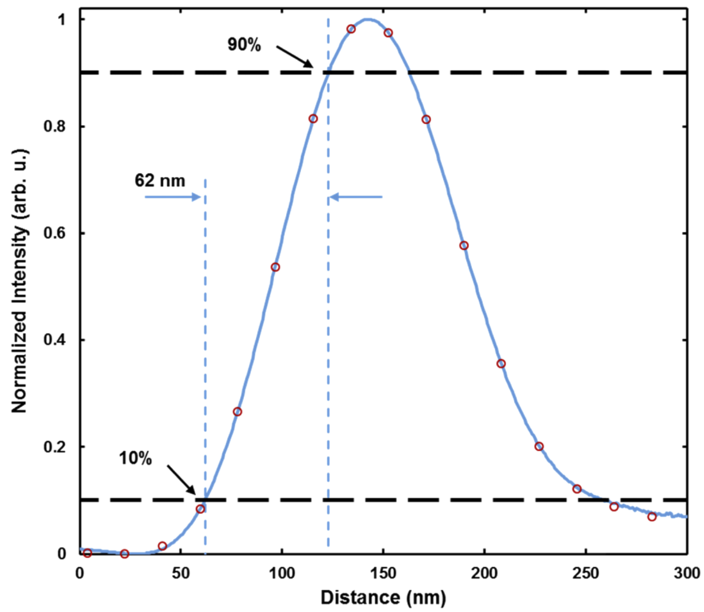

Fig. 8. Characteristic 10% to 90% knife edge cut of the image showing a spatial resolution of 62 nm. The blue line is polynomial fit to the data.

without sacrificing resolution by enlarging the high transmission area where the sample is located while maintaining its distance to the reference pinhole. This could be achieved using a half doughnut shape instead of the circle. The area could also be enlarged by increasing the size of the central opening on the ZP, to create a larger illuminated area. Finally, since the reconstruction of the hologram produces an image of the object at the plane where the reference source is located, it would be possible to inspect the object at different planes along the optical axis by displacing the ZP, which will enable one to compose a tomography of the object.

5. Conclusion

We demonstrated single-shot FTH with ~ 5 ps temporal resolution and up to 62 nm spatial resolution using a highly coherent seeded plasma-based 18.9 nm SXR laser. The field of view achieved covers an area of 38.5 μm^2 that is significantly larger than that of previous experiments. With the recent demonstration of sub 8 nm wavelength gain-saturated plasma-based table-top SXR laser [11] it will be possible to further improve the resolutions both in time and space using compact table-top systems. The single shot capability and rapid FFT reconstruction will allow the real-time recording of ultrafast dynamic phenomena at the table-top scale.

Funding

U.S. Department of Energy (DOE), Office of Science (SC), Basic Energy Sciences (BES), Chemical Sciences, Geosciences, and Biosciences Division (DE-FG02-04ER15592).

Acknowledgment

Previous support from Defense Advanced Research Projects Agency (DARPA) grant D16PC00087 is acknowledged. The experiments were conducted at CSU's ALEPH laser facility supported by LaserNet US from U.S. Department of Energy (DOE), Office of Science (SC), Fusion Energy Sciences (FES) (DESC0019076).

Disclosures

The authors declare no conflicts of interest.

References

1. D. Attwood, *Soft X-Rays and Extreme Ultraviolet Radiation* (Cambridge University Press, 1999).
2. B. W. J. Mcneil and N. R. Thompson, "X-ray free-electron lasers," Nat. Photonics **4**(12), 814–821 (2010).
3. B. Faatz, N. Baboi, V. Ayvazyan, V. Balandin, W. Decking, S. Duesterer, H. J. Eckoldt, J. Feldhaus, N. Golubeva, M. Koerfer, T. Laarmann, A. Leuschner, L. Lilje, T. Limberg, D. Noelle, F. Obier, A. Petrov, E. Ploenjes, K. Rehlich, H. Schlarb, B. Schmidt, M. Schmitz, S. Schreiber, H. Schulte-Schrepping, J. Spengler, M. Staack, F. Tavella, K. Tiedtke, M. Tischer, R. Treusch, A. Willner, J. Bahrdt, R. Follath, M. Gensch, K. Holldack, A. Meseck, R. Mitzner, M. Drescher, V. Miltchev, J. Rönsch-Schulenburg, and J. Rossbach, "FLASH II: A seeded future at FLASH," in *IPAC 2010 - 1st International Particle Accelerator Conference* (2010), pp. 2152–2154.
4. B. D. Patterson, R. Abela, H.-H. Braun, U. Flechsig, R. Ganter, Y. Kim, E. Kirk, A. Oppelt, M. Pedrozzi, S. Reiche, L. Rivkin, T. Schmidt, B. Schmitt, V. N. Strocov, S. Tsujino, and A. F. Wrulich, "Coherent science at the SwissFEL x-ray laser," New J. Phys. **12**(3), 035012 (2010).
5. E. Allaria, L. Badano, S. Bassanese, F. Capotondi, D. Castronovo, P. Cinquegrana, M. B. Danailov, G. D'Auria, A. Demidovich, R. De Monte, G. De Ninno, S. Di Mitri, B. Diviacco, W. M. Fawley, M. Ferianis, E. Ferrari, G. Gaio, D. Gauthier, L. Giannessi, F. Iazzourene, G. Kurdi, N. Mahne, I. Nikolov, F. Parmigiani, G. Penco, L. Raimondi, P. Rebernik, F. Rossi, E. Roussel, C. Scafuri, C. Serpico, P. Sigalotti, C. Spezzani, M. Svandrlik, C. Svetina, M. Trovó, M. Veronese, D. Zangrando, and M. Zangrando, "The FERMI free-electron lasers," J. Synchrotron Radiat. **22**(3), 485–491 (2015).
6. S. Chatziathanasiou, S. Kahaly, E. Skantzakis, G. Sansone, R. Lopez-Martens, S. Haessler, K. Varju, G. D. Tsakiris, D. Charalambidis, and P. Tzallas, "Generation of attosecond light pulses from gas and solid state media," Photonics **4**(4), 26 (2017).
7. J. J. Rocca, "Table-top soft x-ray lasers," Rev. Sci. Instrum. **70**(10), 3799–3827 (1999).
8. Y. Wang, E. Granados, F. Pedaci, D. Alessi, B. Luther, M. Berrill, and J. J. Rocca, "Phase-coherent, injection-seeded, table-top soft-X-ray lasers at 18.9 nm and 13.9 nm," Nat. Photonics **2**(2), 94–98 (2008).
9. D. Alessi, Y. Wang, B. M. Luther, L. Yin, D. H. Martz, M. R. Woolston, Y. Liu, M. Berrill, and J. J. Rocca, "Efficient Excitation of Gain-Saturated Sub-9-nm-Wavelength Tabletop Soft-X-Ray Lasers and Lasing Down to 7.36 nm," Phys. Rev. X **1**(2), 021023 (2011).
10. A. Depresseux, E. Oliva, J. Gautier, F. Tissandier, J. Nejdl, M. Kozlova, G. Maynard, J. P. Goddet, A. Tafzi, A. Lifschitz, H. T. Kim, S. Jacquemot, V. Malka, K. Ta Phuoc, C. Thaury, P. Rousseau, G. Iaquaniello, T. Lefrou, A. Flacco, B. Vodungbo, G. Lambert, A. Rousse, P. Zeitoun, and S. Sebban, "Table-top femtosecond soft X-ray laser by collisional ionization gating," Nat. Photonics **9**(12), 817–821 (2015).
11. A. Rockwood, Y. Wang, S. Wang, M. Berrill, V. N. Shlyaptsev, and J. J. Rocca, "Compact gain-saturated x-ray lasers down to 6.85 nm and amplification down to 5.85 nm," Optica **5**(3), 257–262 (2018).
12. G. Vaschenko, F. Brizuela, C. Brewer, M. Grisham, H. Mancini, C. S. Menoni, M. C. Marconi, J. J. Rocca, W. Chao, J. A. Liddle, E. H. Anderson, D. T. Attwood, A. V. Vinogradov, I. A. Artioukov, Y. P. Pershyn, and V. V. Kondratenko, "Nanoimaging with a compact extreme-ultraviolet laser," Opt. Lett. **30**(16), 2095 (2005).
13. C. A. Brewer, F. Brizuela, P. Wachulak, D. H. Martz, W. Chao, E. H. Anderson, D. T. Attwood, A. V. Vinogradov, I. A. Artyukov, A. G. Ponomareko, V. V. Kondratenko, M. C. Marconi, J. J. Rocca, and C. S. Menoni, "Single-shot extreme ultraviolet laser imaging of nanostructures with wavelength resolution," Opt. Lett. **33**(5), 518–520 (2008).
14. F. Brizuela, Y. Wang, C. A. Brewer, F. Pedaci, W. Chao, E. H. Anderson, Y. Liu, K. A. Goldberg, P. Naulleau, P. Wachulak, M. C. Marconi, D. T. Attwood, J. J. Rocca, and C. S. Menoni, "Microscopy of extreme ultraviolet lithography masks with 13.2 nm tabletop laser illumination," Opt. Lett. **34**(3), 271 (2009).
15. F. Brizuela, S. Carbajo, A. Sakdinawat, D. Alessi, D. H. Martz, Y. Wang, B. Luther, K. A. Goldberg, I. Mochi, D. T. Attwood, B. La Fontaine, J. J. Rocca, and C. S. Menoni, "Extreme ultraviolet laser-based table-top aerial image metrology of lithographic masks," Opt. Express **18**(14), 14467–14473 (2010).
16. G. Vaschenko, C. Brewer, F. Brizuela, Y. Wang, M. A. Larotonda, B. M. Luther, M. C. Marconi, J. J. Rocca, C. S. Menoni, E. H. Anderson, W. Chao, B. D. Harteneck, J. A. Liddle, Y. Liu, and D. T. Attwood, "Sub-38 nm resolution tabletop microscopy with 13 nm wavelength laser light," Opt. Lett. **31**(9), 1214–1216 (2006).
17. S. Carbajo, I. D. Howlett, F. Brizuela, K. S. Buchanan, M. C. Marconi, W. Chao, E. H. Anderson, I. Artioukov, A. Vinogradov, J. J. Rocca, and C. S. Menoni, "Sequential single-shot imaging of nanoscale dynamic interactions with a table-top soft x-ray laser," Opt. Lett. **37**(14), 2994–2996 (2012).
18. I. McNulty, J. Kirz, C. Jacobsen, E. H. Anderson, M. R. Howells, and D. P. Kern, "High-resolution imaging by fourier transform X-ray holography," Science **256**(5059), 1009–1012 (1992).
19. J. Miao, P. Charalambous, J. Kirz, and D. Sayre, "Extending the methodology of X-ray crystallography to allow imaging of micrometre-sized non-crystalline specimens," Nature **400**(6742), 342–344 (1999).
20. A. Barty, S. Boutet, M. J. Bogan, S. Hau-Riege, S. Marchesini, K. Sokolowski-Tinten, N. Stojanovic, R. Tobey, H. Ehrke, A. Cavalleri, S. Düsterer, M. Frank, S. Bajt, B. W. Woods, M. M. Seibert, J. Hajdu, R. Treusch, and H. N. Chapman, "Ultrafast single-shot diffraction imaging of nanoscale dynamics," Nat. Photonics **2**(7), 415–419 (2008).

21. A. Ravasio, D. Gauthier, F. R. N. C. Maia, M. Billon, J. P. Caumes, D. Garzella, M. Géléoc, O. Gobert, J. F. Hergott, A. M. Pena, H. Perez, B. Carré, E. Bourhis, J. Gierak, A. Madouri, D. Mailly, B. Schiedt, M. Fajardo, J. Gautier, P. Zeitoun, P. H. Bucksbaum, J. Hajdu, and H. Merdji, "Single-shot diffractive imaging with a table-top femtosecond soft X-ray laser-harmonics source," Phys. Rev. Lett. **103**(2), 028104 (2009).
22. N. C. Monserud, E. B. Malm, P. W. Wachulak, V. Putkaradze, G. Balakrishnan, W. Chao, E. Anderson, D. Carlton, and M. C. Marconi, "Recording oscillations of sub-micron size cantilevers by extreme ultraviolet Fourier transform holography," Opt. Express **22**(4), 4161 (2014).
23. T. Gorkhover, A. Ulmer, K. Ferguson, M. Bucher, F. R. N. C. Maia, J. Bielecki, T. Ekeberg, M. F. Hantke, B. J. Daurer, C. Nettelblad, J. Andreasson, A. Barty, P. Bruza, S. Carron, D. Hasse, J. Krzywinski, D. S. D. Larsson, A. Morgan, K. Mühlig, M. Müller, K. Okamoto, A. Pietrini, D. Rupp, M. Sauppe, G. Van Der Schot, M. Seibert, J. A. Sellberg, M. Svenda, M. Swiggers, N. Timneanu, D. Westphal, G. Williams, A. Zani, H. N. Chapman, G. Faigel, T. Möller, J. Hajdu, and C. Bostedt, "Femtosecond X-ray Fourier holography imaging of free-flying nanoparticles," Nat. Photonics **12**(3), 150–153 (2018).
24. J. Tenboer, S. Basu, N. Zatsepin, K. Pande, D. Milathianaki, M. Frank, M. Hunter, S. Boutet, G. J. Williams, J. E. Koglin, D. Oberthuer, M. Heymann, C. Kupitz, C. Conrad, J. Coe, S. Roy-Chowdhury, U. Weierstall, D. James, D. Wang, T. Grant, A. Barty, O. Yefanov, J. Scales, C. Gati, C. Seuring, V. Srajer, R. Henning, P. Schwander, R. Fromme, A. Ourmazd, K. Moffat, J. J. Van Thor, J. C. H. Spence, P. Fromme, H. N. Chapman, and M. Schmidt, "Time-resolved serial crystallography captures high-resolution intermediates of photoactive yellow protein," Science **346**(6214), 1242–1246 (2014).
25. Y. Lai, Y. Xue, C. Y. Côté, X. Liu, A. Laramée, N. Jaouen, F. Légaré, L. Tian, and J. Liang, "Single-Shot Ultraviolet Compressed Ultrafast Photography," Laser Photonics Rev. **14**(10), 2000122 (2020).
26. S. Eisebitt, J. Lüning, W. F. Schlotter, M. Lörgen, O. Hellwig, W. Eberhardt, and J. Stöhr, "Lensless imaging of magnetic nanostructures by X-ray spectro-holography," Nature **432**(7019), 885–888 (2004).
27. W. F. Schlotter, R. Rick, K. Chen, A. Scherz, J. Stöhr, J. Lüning, S. Eisebitt, C. Günther, W. Eberhardt, O. Hellwig, and I. McNulty, "Multiple reference Fourier transform holography with soft x rays," Appl. Phys. Lett. **89**(16), 163112 (2006).
28. S. Marchesini, S. Boutet, A. E. Sakdinawat, M. J. Bogan, S. Bajt, A. Barty, H. N. Chapman, M. Frank, S. P. Hau-Riege, A. Szöke, C. Cui, D. A. Shapiro, M. R. Howells, J. C. H. Spence, J. W. Shaevitz, J. Y. Lee, J. Hajdu, and M. M. Seibert, "Massively parallel X-ray holography," Nat. Photonics **2**(9), 560–563 (2008).
29. W. F. Schlotter, J. Lüning, R. Rick, K. Chen, A. Scherz, S. Eisebitt, C. M. Günther, W. Eberhardt, O. Hellwig, and J. Stöhr, "Extended field of view soft x-ray Fourier transform holography: toward imaging ultrafast evolution in a single shot," Opt. Lett. **32**(21), 3110 (2007).
30. B. Pfau, C. M. Günther, S. Schaffert, R. Mitzner, B. Siemer, S. Roling, H. Zacharias, O. Kutz, I. Rudolph, R. Treusch, and S. Eisebitt, "Femtosecond pulse X-ray imaging with a large field of view," New J. Phys. **12**(9), 095006 (2010).
31. R. L. Sandberg, A. Paul, D. A. Raymondson, S. Hädrich, D. M. Gaudiosi, J. Holtsnider, R. I. Tobey, O. Cohen, M. M. Murnane, H. C. Kapteyn, C. Song, J. Miao, Y. Liu, and F. Salmassi, "Lensless diffractive imaging using tabletop coherent high-harmonic soft-X-ray beams," Phys. Rev. Lett. **99**(9), 098103 (2007).
32. R. L. Sandberg, C. Song, P. W. Wachulak, D. A. Raymondson, A. Paul, B. Amirbekian, E. Lee, A. E. Sakdinawat, C. La-O-Vorakiat, M. C. Marconi, C. S. Menoni, M. M. Murnane, J. J. Rocca, H. C. Kapteyn, and J. Miao, "High numerical aperture tabletop soft x-ray diffraction microscopy with 70-nm resolution," Proc. Natl. Acad. Sci. U. S. A. **105**(1), 24–27 (2008).
33. M. D. Seaberg, D. E. Adams, E. L. Townsend, D. A. Raymondson, W. F. Schlotter, Y. Liu, C. S. Menoni, L. Rong, C.-C. Chen, J. Miao, H. C. Kapteyn, and M. M. Murnane, "Ultrahigh 22 nm resolution coherent diffractive imaging using a desktop 13 nm high harmonic source," Opt. Express **19**(23), 22470 (2011).
34. R. L. Sandberg, D. A. Raymondson, C. La-o-vorakiat, A. Paul, K. S. Raines, J. Miao, M. M. Murnane, H. C. Kapteyn, and W. F. Schlotter, "Tabletop soft-x-ray Fourier transform holography with 50 nm resolution," Opt. Lett. **34**(11), 1618 (2009).
35. G. K. Tadesse, W. Eschen, R. Klas, V. Hilbert, D. Schelle, A. Nathanael, M. Zilk, M. Steinert, F. Schrempel, T. Pertsch, A. Tünnermann, J. Limpert, and J. Rothhardt, "High resolution XUV Fourier transform holography on a table top," Sci. Rep. **8**(1), 8677 (2018).
36. J. E. Trebes, S. B. Brown, E. M. Campbell, D. L. Matthews, D. G. Nilson, G. F. Stone, and D. A. Whelan, "Demonstration of x-ray holography with an x-ray laser," Science **238**(4826), 517–519 (1987).
37. H. T. Kim, I. J. Kim, C. M. Kim, T. M. Jeong, T. J. Yu, S. K. Lee, J. H. Sung, J. W. Yoon, H. Yun, S. C. Jeon, I. W. Choi, and J. Lee, "Single-shot nanometer-scale holographic imaging with laser-driven x-ray laser," Appl. Phys. Lett. **98**(12), 121105 (2011).
38. E. B. Malm, N. C. Monserud, C. G. Brown, P. W. Wachulak, H. Xu, G. Balakrishnan, W. Chao, E. Anderson, and M. C. Marconi, "Tabletop single-shot extreme ultraviolet Fourier transform holography of an extended object," Opt. Express **21**(8), 9959 (2013).
39. M. Zürch, R. Jung, C. Späth, J. Tümmler, A. Guggenmos, D. Attwood, U. Kleineberg, H. Stiel, and C. Spielmann, "Transverse Coherence Limited Coherent Diffraction Imaging using a Molybdenum Soft X-ray Laser Pumped at Moderate Pump Energies," Sci. Rep. **7**(1), 5314 (2017).
40. W. Chao, B. D. Harteneck, J. A. Liddle, E. H. Anderson, and D. T. Attwood, "Soft X-ray microscopy at a spatial resolution better than 15 nm," Nature **435**(7046), 1210–1213 (2005).

Optics EXPRESS

41. M. Nishikino, M. Tanaka, K. Nagashima, M. Kishimoto, M. Kado, T. Kawachi, K. Sukegawa, Y. Ochi, N. Hasegawa, and Y. Kato, "Demonstration of a soft-x-ray laser at 13.9 nm with full spatial coherence," Phys. Rev. A: At., Mol., Opt. Phys. **68**(6), 061802 (2003).
42. Y. Wang, S. Wang, A. Rockwood, B. M. B. M. Luther, R. Hollinger, A. Curtis, C. Calvi, C. S. C. S. Menoni, and J. J. J. J. Rocca, "0.85 PW laser operation at 3.3 Hz and high-contrast ultrahigh-intensity $\lambda = 400$ nm second-harmonic beamline," Opt. Lett. **42**(19), 3828–3831 (2017).
43. M. Born and E. Wolf, *Principles of Optics: Electromagnetic Theory of Propagation, Interference and Diffraction of Light*, 7th ed. (Cambridge University Press, 1999).
44. L. M. Meng, D. Alessi, O. Guilbaud, Y. Wang, M. Berrill, B. M. Luther, S. R. Domingue, D. H. Martz, D. Joyeux, S. De Rossi, J. J. Rocca, and A. Klisnick, "Temporal coherence and spectral linewidth of an injection-seeded transient collisional soft x-ray laser," Opt. Express **19**(13), 12087–12092 (2011).
45. M. A. Larotonda, Y. Wang, M. Berrill, B. M. Luther, J. J. Rocca, M. M. Shakya, S. Gilbertson, and Z. Chang, "Pulse duration measurements of grazing-incidence-pumped high repetition rate Ni-like Ag and Cd transient soft x-ray lasers," Opt. Lett. **31**(20), 3043 (2006).